Material Science: An Indian Journal

Materials Science
ISSN: 0974-7486

Research | Vol 16 Iss 1

Synthesis of Fe_2O_3 Using *Emblica officinalis* Extract and its Photocatalytic Efficiency

C Malarkodi[1*], Vidhu Malik[1] and S Uma[1]

Materials Chemistry Group, Department of Chemistry, University of Delhi, Delhi-110007, India

[*]**Corresponding author:** C Malarkodi, Materials Chemistry Group, Department of Chemistry, University of Delhi, Delhi-110007, India, Tel: +254721857685; E-mail: cmalarkodi@chemistry.du.ac.in

Received: January 25, 2018; **Accepted:** February 21, 2018; **Published:** February 28, 2018

Abstract

We identified a green method for the synthesis of Fe_2O_3 using the plant extract of the fruit *E. officinalis*. The fresh fruit extract reacted with a solution of ferric chloride at room temperature to form FeOOH initially. Homogeneous Fe_2O_3 crystallites were obtained after 24 h and were confirmed by the presence of prominent reflections in the PXRD pattern. The presence of various aliphatic amines, alkene and primary amines present in the E. officinalis extract is expected to be responsible for the precipitation of FeOOH and subsequent formation of Fe_2O_3. The FTIR spectra of Fe_2O_3 indicated the presence of the bands corresponding to different organic amine and alkene functional groups. The band gap energy of the resultant Fe_2O_3 investigated by the UV-vis absorption spectroscopy was found to be in the range of 1.97-2.05 eV. The photocatalytic efficiency of Fe_2O_3 nanoparticles was evaluated by the degradation of Rhodamine 6G (Rh-6G) under visible light irradiation.

Keywords:* *E. officinalis; Green synthesis; Fe_2O_3 nanoparticles; Photocatalytic activity

Introduction

Metals, bimetallic alloys, binary and ternary metal chalcogenides in nano-size dimensions with well-defined shapes and structures along with unique properties have been widely researched in the past decades because of their vital role in nanotechnology and catalysis [1]. Among the vast majority of materials that are available, Fe_2O_3 deserves special mention because of its easy accessibility with potential applications such as targeted drug delivery, sensors, photo catalysis, and biomedicines and most commonly for water purification etc. [2-7]. The synthesis of Fe_2O_3 in Nano dimensions using naturally occuring reagents available from plants will be significant for special biological related applications. Although many biological based methods are available for the synthesis of magnetic nanoparticles of α-Fe_2O_3 [8], research efforts are continued to find non-toxic, environmental friendly alternate methods [9]. Usually, the reported methods make use of the plant extracts as reagents and some of the previously known plant sources include *Hibiscus rosa sinensis*, *Pisum sativum*, *Psidium guajava*, *Emblica officinalis*, *Aloe vera* extract and *Piper nigrum* [10-15]. TABLE 1 lists the literature data on the various plant reagents that are used for the synthesis of different metal and metal oxide materials [16-31]. *Phyllanthus*

Citation: Malarkodi C, Malik V, Uma S, et al. Synthesis of Fe_2O_3 Using *Emblica officinalis* Extract and its Photocatalytic Efficiency. Mat Sci Ind J. 2018;16(1):125

emblica (Emblica officinalis) commonly known as Indian "gooseberry" or amla, belonging to family Euphorbiaceae is an important herbal drug used in ayurvedic systems of medicine. *E. officinalis* has been reported to play a beneficial role to treat diseases such as diabetes, ulcer, and anemia and possesses cardio protective properties [32]. *E. officinalis* fruit extracts contain chemicals including quercetin, ascorbic acid, gallic acid, tannins, flavonoids, and pectin and polyphenolic compounds [33]. The present work reports the investigation of using *E. officinalis* fruit extracts as a biological reagent for the synthesis of Fe_2O_3. The synthesized Fe_2O_3 has been characterized and explored as a photo catalyst under visible light illumination.

TABLE 1. **List of nanomaterials obtained using plant sources.**

S. No.	Sources (Common name)	Precursor-Product	References
1	***Emblica officinalis*** (Indian goose berry)	$Mg(NO_3)_2$–MgO	16
2	***Eucalyptus leaf extract*** (Tasmanian bluegum)	$FeSO_4 \cdot 7H_2O$–Fe	17
3	***Aspalathus linearis*** (Rooibos tea)	$RuCl_3.H_2O$–RuO_2	18
4	***Cacumen platycladi extract*** (Oriental thuja)	$RhCl_3$–RuO	19
5	***Acalypha indica*** (Indian acalypha)	$CuSO_4$–CuO	20
6	***Tabernaemontana divaricate*** (Crape jasmine)	$CuSO_4$–CuO	21
7	***Thymus vulgaris L*** (Garden thyme)	$CuCl_2$–CuO	22
8	***Allium sativum*** (garlic), ***Allium cepa*** (onion) and ***Petroselinum crispum*** (parsley)	$Zn(NO_3)_2$–ZnO	23
9	***Rosa canina*** (Dog-rose)	$Zn(NO_3)_2$–ZnO	24
10	***Plectranthus amboinicus*** (Indian borage)	$Zn(NO_3)_2$–ZnO	25
11	***Azadirachta indica*** (*Neem*)	$Zn(Ac)_2$–ZnO	26
12	***Sargassum muticum*** (Japanese wireweed)	$Zn(Ac)_2$–$2H_2O$)–ZnO	27
13	***Trifolium pretense*** (Beebread)	$Zn(Ac)_2$–ZnO	28
14	***Callistemon viminalis*** (Weeping Bottlebrush)	$[Sm(CH_3COO)_3(H_2O)_2]$ –Sm_2O_3	29
15	***Hibiscus sabdariffa*** (Roselle)	$Ce(NO_{3)3}$–CeO	30
16	***Pseudokirchneriella subcapitata*** (Selenstrum capriconutum)	$Ce(NO_3)_4$–CeO_2	31

Materials and Methods

Collection and preparation of plant extract

The fruits sample of *E. officinalis* was collected from the local market near Mayur vihar phase III, New Delhi, India.

Fresh extract

E. officinalis fruit extract was prepared following a procedure reported earlier [13]. *E. officinalis* fruits were thoroughly washed with water and finely chopped. The *E. officinalis* fruit pieces were then crushed into the mortar and pestle through the deionized water in a mass to volume ratio 10 g of fruit pieces to 100 ml of water. The mixture was allowed to stand for 10 minutes and passed through the Whatman No.1 filter paper to remove the solids parts. The filtrate was stored at 4°C and was used for the synthesis.

Boiled extract

10 g of finely chopped *E. officinalis* fruits was weighed and boiled with 100 ml of double distilled water at 60°C-80°C for 10 minutes. After boiling, the solution was filtered through the Whatman No. 1 filter paper and stored at 4°C for further use.

Reflux condition

10 g of *E. officinalis* fruits were chopped and refluxed with 100 ml of double distilled water for 1 h, followed by filtering and storing at 4°C for further use.

Synthesis of Fe_2O_3 nanoparticles using *E. officinalis* extracts

Synthesis of Fe_2O_3 nanoparticles was carried out using fresh extract of *E. officinalis* obtained by boiling and reflux procedures as detailed above. 0.4055 g of $FeCl_3$ (1 mM) was dissolved in 90 ml of double distilled water. 10 ml of *E. officinalis* was added separately to this 90 ml of aqueous solution of $FeCl_3$. The reaction mixtures were stirred for 5 h at room temperature with the formation of brick red color colloidal Fe_2O_3 particles at the bottom of the flask which were allowed to stand for 24 h. The colloidal solution was centrifuged at 2000 rpm for 20 minutes and washed with double distilled water repeatedly to remove any impurities followed by drying in hot air oven at 60°C for 5 h (FIG. 1).

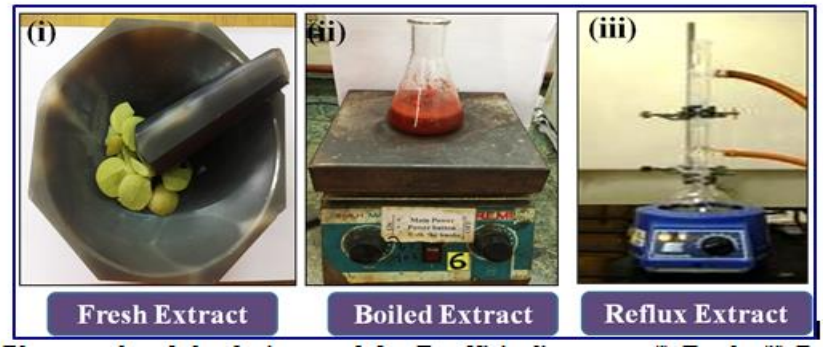

FIG. 1. **Photographs of the devices used for *E. officinalis* extract (i) Fresh (ii) Boiled and (iii) Reflux.**

Synthesis of Fe_2O_3 nanoparticles using ascorbic acid

In a typical experiment, 0.4055 g of $FeCl_3$ (1 mM) was dissolved in 90 ml of double distilled water continuously stirring to form a red solution, and then, 10 ml of 0.4 g ascorbic acid was added to the solution slowly. The reaction mixtures were stirred for 5 h at room temperature with the formation of brick red color colloidal Fe_2O_3 particles at the bottom of the flask which were allowed to stand for 24 h. The colloidal solution was centrifuged at 2000 rpm for 20 minutes and washed with double distilled water repeatedly to remove any impurities followed by drying in hot air oven at 60°C for 5 h.

Characterization

High resolution X'Pert PANanalytical diffractometer equipped with a Xe Propotional detector employing Cu Kα radiation (λ=1.5418 Å) was employed to obtain data with a scan rate of 1.65 s per step and with a step size of 0.04°C at 298 K (DY3813). The SEM micrograph of the sample was recorded using JEOL 6610 LV. TEM was obtained using FEI Technai G2 20 electron microscope operating at 200 kV. Fourier Transform Infra-Red spectroscopy was recorded using a Perkin Elmer 2000 spectrometer using KBr pellet technique. UV-vis diffuse reflectance data were collected over the spectral range 200−800 nm using Perkin-Elmer Lambda 35 (Waltham, MA, USA) scanning double beam spectrometer equipped with a 50 mm integrating sphere. The data were transformed into absorbance with the Kubelka-Munk function for the estimation of the band gap. The synthesized Fe_2O_3 has been characterized and explored as a photocatalyst for the degradation of the cationic dye Rhodamine 6G (Rh-6G) under visible light illumination of a 450 W xenon lamp. The details of the photocatalytic set up have been described earlier [34]. 0.1g of catalyst was added to 50 ml aqueous solution of solution of Rh-6G (10-5 M Concentration). Before the measurements, the suspension was stirred in dark for 30 mins to achieve an adsorption-desorption equilibrium. After shining the light, 4 ml of solution was collected at 1 h intervals and the catalyst was separated using centrifugation. The degradation was followed by monitoring decrease in the λ_{max} (540 nm) of Rh–6G.

Results and Discussion

The formation of Fe_2O_3 nanoparticles of the filtrate was primarily followed by carefully observing the color change during the reaction. The appearance of brick red color after the treatment of clear yellow $FeCl_3$ solution with the extract of *E. officinalis* fruit suggested possible reaction. FIG. 2 (i) shows the digital photographs of the solution of *E. officinalis* fruit extract with added $FeCl_3$ solution together with the blank $FeCl_3$ solution in which fruit extract was not added. The color change from yellow to red was observed within 2-10 mins after mixing and after 6-12 h the suspended particles in the solution got settled down at the bottom of the flask. The stability of the brick red color crystallites after 24 h suggested the formation of Fe_2O_3 possibly from FeOOH that gets precipitated initially. The biomolecule interaction is expected since the hydroxide followed by oxide generation requires change in pH [35]. The PXRD patterns of Fe_2O_3 nanoparticles synthesize using *E. officinalis* extracts along with Fe_2O_3 synthesized independently using ascorbic acid are shown in FIG. 2 (ii) and (iii).

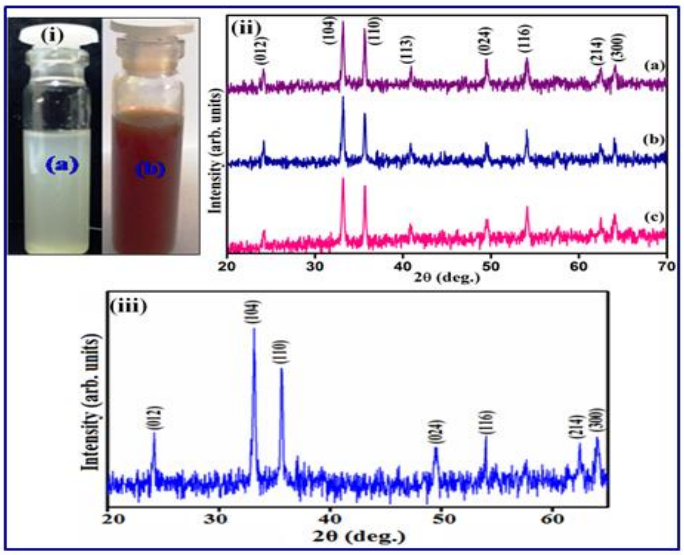

FIG. 2. **(i) Photographs of *E. officinalis* extract (a) before and (b) after addition of $FeCl_3$, (ii) PXRD pattern of Fe_2O_3 synthesized using (a) fresh (b) boiled (c) reflux extract and (iii) Fe_2O_3 synthesized using ascorbic acid.**

The observed reflections were indexed in rhombohedral symmetry with lattice parameters a=5.035 (5) Å and c=13.74 (7) Å (S.G. $R\bar{3}c$) and matched with the reported pattern (JCPDS File No. 86-0550) [36]. The XRD pattern of these peaks reveals that the Fe_2O_3 nanoparticles are crystalline in nature. SEM images coupled with TEM revealed the aggregation of rod shaped of Fe_2O_3 crystallite with diameter ranging between 20 nm to 100 nm (FIG. 3).

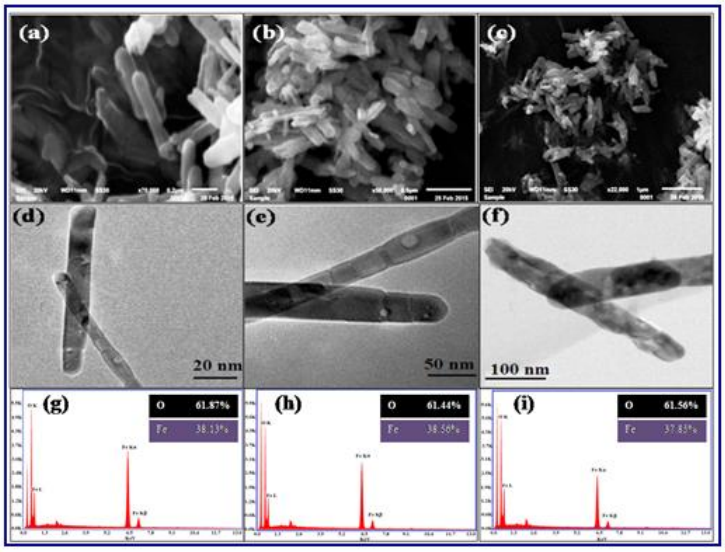

FIG. 3. **SEM, TEM images and EDX spectrum of Fe_2O_3 nanoparticles synthesized using (a, d and g) fresh, (b, e and h) boiled and (c, f and i) reflux extract.**

Fe_2O_3 nanoparticles synthesized using *E. officinalis* fresh extracts have more uniform distribution, while boiled and refluxed *E. officinalis* extracts produced much larger aggregation of the Fe_2O_3 particles. The elemental compositional analysis of the

synthesized Fe_2O_3 was also confirmed using EDX. The FTIR spectra of Fe_2O_3 obtained using different *E. officinalis* extracts indicated the presence of finger print bands corresponding to aliphatic amine, alkene and primary amines (FIG. 4 (i)). The band in the region of 3436 cm^{-1} is ascribed to the N-H stretching vibrations of primary amines (R-NH2). The bands at 2934 and 2856 cm^{-1} are due to the presence of C-H bonds. Thus, FTIR results confirm the presence of primary amines that are mostly responsible for the formation of Fe_2O_3 particles. The presence of 1056 and 1457 cm^{-1} can be assigned to C-O and C-C stretching of alcohols respectively [37,38]. Finally the bands due to Fe-O stretching at 536 and 454 cm^{-1} were also observed. The UV-visible diffuse reflectance spectrum consisted of the strong absorption of Fe_2O_3 at 530 nm (FIG. 4 (ii)). The band gap energy was evaluated by plotting the Kubelka-Munk function with photon energy (eV) and was found to vary from 1.97-2.05 eV and these observed values were in close agreement with the earlier reported [39].

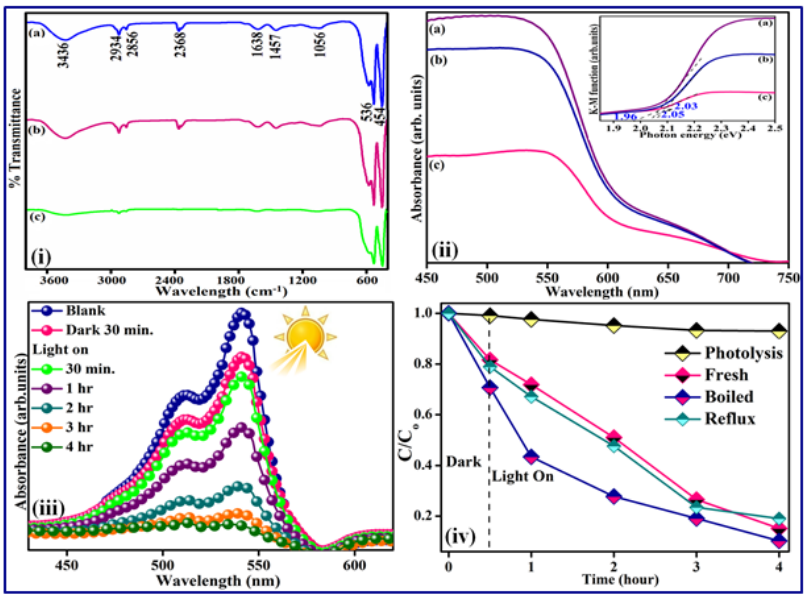

FIG. 4**. (i) FTIR-Spectrum and (ii) UV-visible diffuse reflectance spectra (inset shows plots of Kubelka-Munk Function versus photon energy (eV)) of synthesized Fe_2O_3 nanoparticles using (a) fresh (b) boiled and (c) refluxed extract, (iii) Photocatalytic degradation of Rh-6G using Fe_2O_3 nanoparticles and (iv) shows the respective C/Co vs. time plots of Rh-6G.**

The photocatalytic activity of Fe_2O_3 synthesized using fresh, boiled and reflux extract were evaluated for the degradation of aqueous Rh-6G under visible 400 nm<λ>800 nm radiation. The concentration of the dye solution was not decreased in the presence of the catalysts in dark. Also, photolysis of the dye solution under light irradiation was carried out without the addition of the catalysts in order to separate the noticeable degradation due to photo catalysis by the catalysts under visible light irradiation. The fact that only negligible decrease occurred in the concentration of the dye in the absence of the catalyst, suggested that certainly photo catalysis has taken place in the presence of Fe_2O_3 catalyst within four hours under visible light irradiation as shown by the decrease in the absorbance intensity at 540 nm. Appreciable decomposition was noticed only by photocatalysis using Fe_2O_3 under visible light (FIG. 4(iii)). Further, the Fe_2O_3 obtained using boiled extract showed better photocatalytic abilities as compared to the Fe_2O_3 obtained using the fresh or refluxed *E. officinalis* extracts (FIG. 4(iv)).

Conclusion

Fe_2O_3 nanoparticles have been successfully synthesized using the extract obtained from *E. officinalis* and the formation was confirmed by a variety of analytical techniques. This approach offers a novel ecofriendly and cost effective method probably. The extract containing possibly different stabilizing and capping agents is responsible for the formation of Fe_2O_3 from ferric chloride solution. Fe_2O_3 nanocrystallites are found to be useful to degrade aqueous solution of Rh-6G under visible light irradiation.

Acknowledgements

Authors thank DST (SR/S1/PC-07/2011), DU-DST Purse Grant phase-II and University of Delhi under the "Scheme to Strengthen RandD Doctoral Research Program". Timely help from Prof. R. Nagarajan for encouragement is profusely acknowledged. CM and VM thank UGC woman PDF and CSIR for SPMF fellowship respectively.

REFERENCES

1. Diodati S, Dolcet P, Casarin M, et al. Pursuing the crystallization of mono and polymetallic nanosized crystalline inorganic compounds by low-temperature wet-chemistry and colloidal routes. Chem Rev. 2015;115(20):11449-502.
2. Yang L, Cao Z, Sajja HK, et al. Development of receptor targeted magnetic iron oxide nanoparticles for efficient drug delivery and tumor imaging. J Biomed Nanotechnol. 2008;4(4):439-49.
3. Drbohlavova J, Hrdy R, Adam V, et al. Preparation and properties of various magnetic nanoparticles. Sensors (Basels). 2009;9(4):2352-62.
4. Wang C, Huang Z. Controlled synthesis of α-Fe_2O_3 nanostructures for efficient photocatalysis. Mater Lett. 2016;164:194-7.
5. Zeng J, Li J, Zhong J, et al. Improved Sun light photocatalytic activity of α-Fe_2O_3 prepared with the assistance of CTAB. Mater Lett. 2015;160:526-8.
6. Ren T, He P, Niu W, et al. Synthesis of α-Fe_2O_3 nanofibers for applications in removal and recovery of Cr (VI) from wastewater. Environ Sci Pollut Res Int. 2013;20(1):155-62.
7. Pankhurst QA, Connolly J, Jones SK, et al. Applications of magnetic nanoparticles in biomedicine. J Phys D. 2003;36(13):R167.
8. Sarkar J, Mollick MM, Chattopadhyay D, et al. An eco-friendly route of γ-Fe_2O_3 nanoparticles formation and investigation of the mechanical properties of the HPMC-γ-Fe_2O_3 nanocomposites. Bioprocess Biosyst Eng. 2017;40(3):351-9.
9. Saif S, Tahir A, Chen Y. Green synthesis of iron nanoparticles and their environmental applications and implications. Nanomaterials. 2016;6(11):209.

10. Manikandan A, Durka M, Antony SA. *Hibiscus rosa-sinensis* leaf extracted green methods, magneto-optical and catalytic properties of spinel $CuFe_2O_4$ nano-and microstructures. J Inorg Organomet Polym Mater. 2015;25(5):1019-31.
11. Mukherjee A, Pokhrel S, Bandyopadhyay S, et al. A soil mediated phyto-toxicological study of iron doped zinc oxide nanoparticles (Fe@ ZnO) in green peas (*Pisum sativum* L.). Chem Eng J. 2014;258:394-401.
12. Santhoshkumar T, Rahuman AA, Jayaseelan C, et al. Green synthesis of titanium dioxide nanoparticles using *Psidium guajava* extract and its antibacterial and antioxidant properties. Asian Pac J Trop Med. 2014;7(12):968-76.
13. Ramesh PS, Kokila T, Geetha D. Plant mediated green synthesis and antibacterial activity of silver nanoparticles using *Emblica officinalis* fruit extract. Spectrochim Acta A. 2015;142:339-43.
14. Manikandan A, Sridhar R, Antony SA, et al. A simple aloe vera plant-extracted microwave and conventional combustion synthesis: Morphological, optical, magnetic and catalytic properties of $CoFe_2O_4$ nanostructures. J Mol Struct. 2014 ;1076:188-200.
15. Mohapatra B, Kuriakose S, Mohapatra S. Rapid green synthesis of silver nanoparticles and nanorods using *Piper nigrum* extract. J Alloys Compd. 2015;637:119-26.
16. Ramesh PS, Kokila T, Geetha D. Plant mediated green synthesis and antibacterial activity of silver nanoparticles using *Emblica officinalis* fruit extract. Spectrochim. Acta A. 2015;142:339-43.
17. Zhuang Z, Huang L, Wang F, et al. Effects of cyclodextrin on the morphology and reactivity of iron-based nanoparticles using Eucalyptus leaf extract. Ind Crops Prod. 2015 ;69:308-13.
18. Ismail E, Diallo A, Khenfouch M, et al. RuO_2 nanoparticles by a novel green process via *Aspalathus linearis* natural extract and their water splitting response. J Alloys Compd. 2016;662:283-9.
19. Huang Y, Ma Y, Cheng Y, et al. Biosynthesis of ruthenium nanoparticles supported on nitric acid modified activated carbon for liquid-phase hydrogenation of 2, 2, 4, 4-tetramethylcyclobutane-1, 3-dione. Catal Commun. 2015 Dec 5;72:20-3.
20. Sivaraj R, Rahman PK, Rajiv P, et al. Biosynthesis and characterization of *Acalypha indica* mediated copper oxide nanoparticles and evaluation of its antimicrobial and anticancer activity. Spectrochim Acta A. 2014;129:255-8.
21. Sivaraj R, Rahman PK, Rajiv P, et al. Biogenic copper oxide nanoparticles synthesis using *Tabernaemontana divaricate* leaf extract and its antibacterial activity against urinary tract pathogen. Spectrochim Acta A. 2014;133:178-81.

22. Nasrollahzadeh M, Sajadi SM, Rostami-Vartooni A, et al. Green synthesis of CuO nanoparticles using aqueous extract of *Thymus vulgaris* L. leaves and their catalytic performance for N-arylation of indoles and amines. J Colloid Interface Sci. 2016;466:113-9.
23. Stan M, Popa A, Toloman D, et al. Enhanced photocatalytic degradation properties of zinc oxide nanoparticles synthesized by using plant extracts. Mater Sci Semicond Process. 2015;39:23-9.
24. Jafarirad S, Mehrabi M, Divband B, et al. Biofabrication of zinc oxide nanoparticles using fruit extract of *Rosa canina* and their toxic potential against bacteria: A mechanistic approach. Mater Sci Eng C. 2016;59:296-302.
25. Fu L, Fu Z. *Plectranthus amboinicus* leaf extract-assisted biosynthesis of ZnO nanoparticles and their photocatalytic activity. Ceram Int. 2015;41(2):2492-6.
26. Bhuyan T, Mishra K, Khanuja M, et al. Biosynthesis of zinc oxide nanoparticles from *Azadirachta indica* for antibacterial and photocatalytic applications. Mater Sci Semicond Process. 2015;32:55-61.
27. Azizi S, Ahmad MB, Namvar F, et al. Green biosynthesis and characterization of zinc oxide nanoparticles using brown marine macroalga *Sargassum muticum* aqueous extract. Mater Lett. 2014;116:275-7.
28. Dobrucka R, Długaszewska J. Biosynthesis and antibacterial activity of ZnO nanoparticles using Trifolium pratense flower extract. Saudi J Biol Sci. 2016;23(4):517-23.
29. Sone BT, Manikandan E, Gurib-Fakim A, et al. Sm_2O_3 nanoparticles green synthesis via Callistemon viminalis' extract. J Alloys Compd. 2015;650:357-62.
30. Thovhogi N, Diallo A, Gurib-Fakim A, et al. Nanoparticles green synthesis by Hibiscus Sabdariffa flower extract: main physical properties. J Alloys Compd. 2015;647:392-6.
31. Booth A, Størseth T, Altin D, et al. Freshwater dispersion stability of PAA-stabilised cerium oxide nanoparticles and toxicity towards *Pseudokirchneriella subcapitata*. Sci Total Environ. 2015;505:596-605.
32. Khan KH. Roles of *Emblica officinalis* in medicine-A review. Botany Research International. 2009;2(4):218-28.
33. Hossain MM, Mazumder K, Hossen SM, et al. *In vitro* studies on antibacterial and antifungal activities of *Emblica officinalis*. Int J Pharm Sci Res. 2012;3(4):1124.
34. J Singh, S Uma. Efficient photocatalytic degradation of organic compounds by ilmenite $AgSbO_3$ under visible and UV light irradiation. J Phys Chem. 2009;113:12483.
35. Pardha-Saradhi P, Yamal G, Peddisetty T, et al. Plants fabricate Fe-nanocomplexes at root surface to counter and phytostabilize excess ionic Fe. Biometals. 2014;27(1):97-114.
36. Ahmmad B, Leonard K, Islam MS, et al. Green synthesis of mesoporous hematite (α-Fe_2O_3) nanoparticles and their photocatalytic activity. Adv Polym Tech. 2013;24(1):160-7.

37. Ramanujam K, Sundrarajan M. Antibacterial effects of biosynthesized MgO nanoparticles using ethanolic fruit extract of *Emblica officinalis*. J Photochem Photobiol. 2014;141:296-300.
38. Mohamed GF, Shaheen MS, Khalil SK, et al. Application of FT-IR spectroscopy for rapid and simultaneous quality determination of some fruit products. Nat Sci. 2011;9(11):21-31.
39. Xia C, Jia Y, Tao M, et al. Tuning the band gap of hematite α-Fe_2O_3 by sulfur doping. Phys Lett. 2013;377(31-33):1943-7.